ELSEVIER

Journal of Photochemistry and Photobiology A: Chemistry 139 (2001) 225–232

Journal of Photochemistry and Photobiology A:Chemistry

www.elsevier.nl/locate/jphotochem

Prediction of primary intermediates and the photodegradation kinetics of 3-aminophenol in aqueous TiO_2 suspensions

Nevim San, Arzu Hatipoğlu, Gülin Koçtürk, Zekiye Çınar*

Department of Chemistry, Yildiz Technical University, 34210 Istanbul, Turkey

Received 15 December 2000; accepted 23 December 2000

Abstract

The kinetics of the photocatalytic degradation of 3-aminophenol (3-AP) has been investigated experimentally and theoretically. The reactions have been carried out in a batch-type photoreactor using TiO_2 P25 Degussa as the photocatalyst. The effects of the catalyst loading, the initial concentration of 3-AP and the electron acceptors; H_2O_2, $K_2S_2O_8$ and $KBrO_3$ on the degradation rate have been determined. With the intention of predicting the primary intermediates, geometry optimizations of the reactants, products and the transition state complexes have been performed with the semi-empirical PM3 method. The molecular orbital calculations have been carried out by an SCF method using RHF or UHF formalisms. Based on the results of the quantum mechanical calculations, the rate constants of the four possible reaction paths have been calculated by means of the Transition State Theory and 1,4-dihydroxy-3-amino-cyclohexa-2,5-dienyl radical has been determined as the most probable primary intermediate.

Keywords: Photocatalytic degradation; Titanium dioxide; 3-Aminophenol; Semi-empirical PM3 method; Electron acceptors

1. Introduction

Heterogeneous photocatalysis is a promising new technique to destroy organic pollutants in water. In the past two decades, extensive research has been done on this subject and the process has recently been reviewed [1–3]. Heterogeneous photocatalysis is based on the combined use of light and semiconductors, generally the anatase form of TiO_2 [4,5]. When TiO_2, an n-type semiconductor is irradiated with light of wavelength $\lambda \leq 390$ nm, electron (e^-)–hole (h^+) pairs are produced. In the presence of oxygen, these pairs migrate to the interface to yield oxidizing species. In aqueous suspension systems, electrons are trapped at surface defect sites (Ti^{3+}) and removed by reactions with adsorbed molecular O_2 to produce superoxide anion radical, $O_2{}^{-\bullet}$, whereas holes react with surface OH^- groups and produce $^\bullet$OH radicals which are the most oxidizing species of this process [6–9].

Aromatic compounds constitute an important class of water pollutants because of their stability and solubility in water. Most of them are known to withstand biodegradation and chemical oxidation methods are expensive [10,11]. Thus, heterogeneous photocatalysis seems to be more effective than the conventional methods because semiconductors are inexpensive and capable of mineralizing various aromatic compounds. Phenol and its derivatives, especially halogenated phenols, are the most widely studied aromatics because of their environmental importance. Nitrogen-containing aromatics are also of great concern, not only because they cause severe health problems but, at the same time they are important poisons for catalysts [12]. Many aromatic compounds are known to be converted to CO_2, H_2O and small molecules, depending upon the types of substituents and their photocatalytic disappearance rates have been measured [7–13]. However, there is very limited information on the kinetics of the photocatalytic degradation of nitrogen-containing aromatics [14–16].

In this study, 3-aminophenol (3-AP) was chosen as the representative member of this pollutant group, because of its unusual structure; –OH group is *ortho-*, *para-* directing but $–NH_2$ is at the *meta-* position with respect to it. The 3-AP is toxic as are the other phenol derivatives. It is an allergen and skin irritant. The 3-AP is a dye intermediate and a very important compound in pharmaceutical industry. Since it has a significant water solubility, 2.6 g/100 ml, it is often present in wastewater discharges from such facilities. It may also be found in ground water wells and surface waters where it has to be removed in order to achieve drinking water quality.

In this paper, we present the results of our investigation on the photodegradation kinetics of 3-AP in aqueous TiO_2

* Corresponding author. Tel.: +90-212-449-1844; fax: +90-216-348-6652.
E-mail address: cinarz@yildiz.edu.tr (Z. Çınar).

1010-6030/01/$ – see front matter
PII: S1010-6030(01)00368-9

suspensions. In the first part of the work, the effects of catalyst loading, initial concentration of 3-AP and the electron acceptors namely; H_2O_2, $K_2S_2O_8$ and $KBrO_3$ were determined experimentally. In the theoretical part, with the intention of predicting the types and the relative amounts of the primary intermediates, quantum mechanical calculations were carried out for all the possible reaction paths.

2. Experimental details

2.1. Materials

The anatase form of TiO_2, Degussa P25 grade, with a particle size of 30 nm and a surface area of $50\,m^2\,g^{-1}$ was used as the photocatalyst without further treatment. All the chemicals that were used in the experiments were of laboratory reagent grade and used as received without further purification. The solutions were prepared with doubly distilled water.

2.2. Photoreactor

The experiments were carried out in a batch-type photoreactor. The reactor consists of two parts. The first part is the outside metallic cylinder, which is 54.4 cm high and 31.6 cm in inside diameter. There are 5×8 W blacklight fluorescent lamps attached vertically onto the inner surface of the metallic cylinder at a distance of 12.0 cm apart from each other. At the bottom of the outer cylinder, there is a fan to cool the lamps. The second part of the reactor is a Pyrex glass cylinder which is 18.3 cm high and 9.0 cm in inside diameter with a volume of approximately 1000 ml and was used as the reaction vessel. The suspension was stirred magnetically throughout the reaction period in order to prevent TiO_2 particles from settlement. The incident light intensity was measured by means of a potassium ferrioxalate actinometer [17] and found to be 3.1×10^{-7} einsteins s^{-1}.

2.3. Experiments

In the experiments, a stock solution of 3-AP at a concentration of $1.0 \times 10^{-4}\,mol\,l^{-1}$ was used. The suspension was prepared by mixing definite volumes of this solution containing the desired amount of 3-AP with TiO_2. The suspension was agitated in an ultrasonic bath for 15 min in the dark before introducing into the photoreactor. The volume of the suspension was 600 ml. In most of the experiments, the amount of TiO_2 used was 0.3 g/100 ml which was determined as the optimum photocatalyst concentration. Owing to continuous cooling, the temperature of the reaction solution was $22 \pm 2°C$. Under these conditions, the initial pH of the suspension was 5.3 ± 0.2 and measured by a pH-meter, Metrohm E-510.

All the samples, each 10 ml in volume were taken intermittently for analysis. The samples were then filtered through 0.45 μm Millipore discs. Before analyzing, all the solutions were wrapped with aluminium foil and kept in the dark. The concentration of 3-AP was measured with a Unicam UV-Visible spectrophotometer. The calibration curves were prepared for a concentration range of $(1.0–10.0) \times 10^{-5}\,mol\,l^{-1}$ and the detection limit for 3-AP was calculated to be $3.82 \times 10^{-6}\,mol\,l^{-1}$. In the experiments, the pH of the reaction solution decreased slightly. For 160 min of degradation, the change in the pH was 0.1–0.2 which did not affect the wavelength of maximum absorption in the UV-spectrum of 3-AP.

3. Results and discussion

3.1. Kinetics of 3-AP disappearance

Fig. 1 shows the kinetics of the disappearance of 3-AP from an initial concentration of $1.0 \times 10^{-4}\,mol\,l^{-1}$ under three conditions. There was no observable loss of 3-AP when the irradiation was carried out in the absence of TiO_2. In unirradiated suspensions, there was a slight loss, ca. 4.9%, due to adsorption onto TiO_2 particles. However, in the presence of TiO_2, a rapid degradation of 3-AP occurred by irradiation. The concentration change amounts to 52.8% after irradiating for 160 min.

The semilogarithmic plots of concentration data gave a straight line. The correlation constant for the fitted line is $r = 0.9953$. This finding indicates that the photocatalytic degradation of 3-AP in aqueous TiO_2 suspensions can be described by the first-order kinetic model, $\ln C = -kt + \ln C_0$, where C_0 is the initial concentration and C is the concentration of 3-AP at time t. Under the experimental conditions used, the rate constant k for the degradation of 3-AP was calculated to be $(5.06 \pm 0.16) \times 10^{-3}\,min^{-1}$.

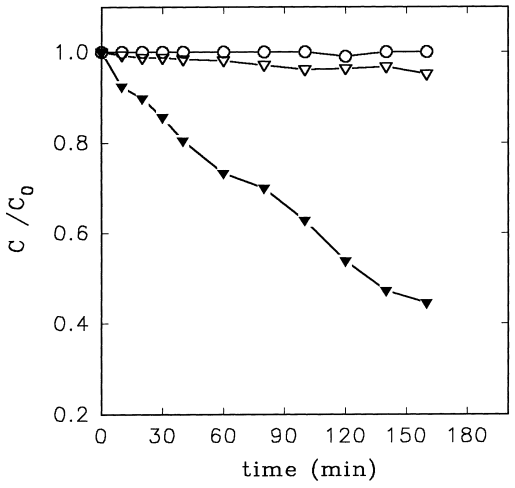

Fig. 1. Photocatalytic disappearance of 3-AP ((○) with light, (▽) with TiO_2, (▼) with TiO_2 + light).

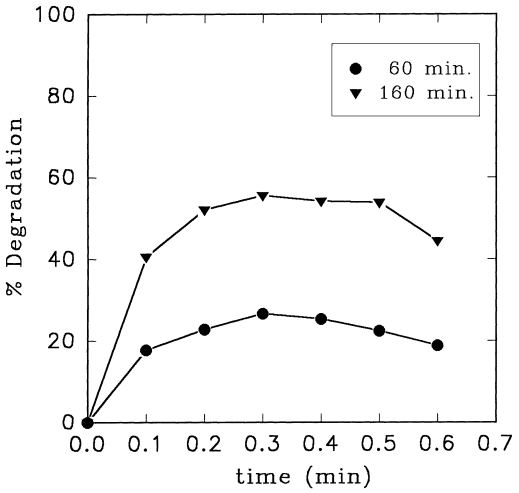

Fig. 2. Effect of TiO_2 loading on the photodegradation rate of 3-AP.

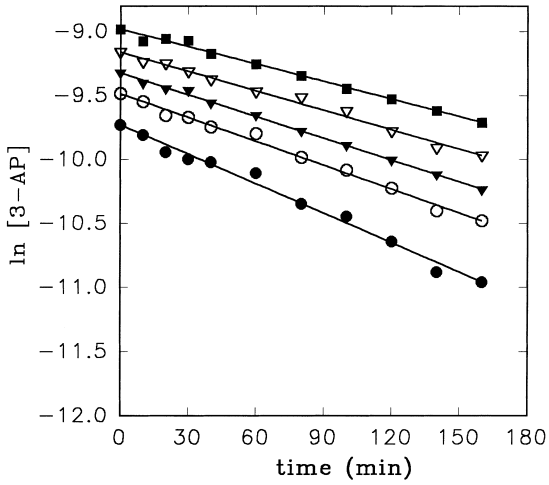

Fig. 3. Effect of initial concentration on the photodegradation rate of 3-AP ((●) 5.9×10^{-5} mol l^{-1}, (○) 7.6×10^{-5} mol l^{-1}, (▼) 8.9×10^{-5} mol l^{-1}, (▽) 10.5×10^{-5} mol l^{-1}, (■) 12.6×10^{-5} mol l^{-1}).

3.2. Effect of catalyst loading

Suspensions at pH $= 5.3 \pm 0.2$ and 1.0×10^{-4} mol l^{-1} 3-AP concentration were used to study the effect of catalyst loading by varying the amount of TiO_2 from 0.1 to 0.6 g/100 ml. The effect of TiO_2 concentration on the degradation of 3-AP is presented in Fig. 2 for two different irradiation times, 60 and 160 min. Both of the curves show that without catalyst, the degradation of 3-AP is insignificant. As the concentration of TiO_2 increases, the rate of degradation increases upto a certain point, then begins to decrease slowly. Maximum degradation was obtained at a TiO_2 concentration of 0.3 g/100 ml. This observation indicates that beyond this optimum concentration, other factors affect the degradation of 3-AP. At high TiO_2 concentrations, particles aggregate which reduces the interfacial area between the reaction solution and the catalyst, thus, they decrease the number of active sites on the surface. Light scattering by the particles and the increase in opacity may be other reasons for the decrease in the degradation rate.

3.3. Effect of initial concentration of 3-AP

Since the pollutant concentration is a very important parameter in water treatment, the effect of initial 3-AP concentration was investigated over the concentration range of (6.0–12.6) $\times 10^{-5}$ mol l^{-1}. Experimental results are presented in Fig. 3 and in Table 1, together with the correlation coefficients r for each of the fitted lines. The results show that the degradation rate depends on the initial 3-AP concentration. The rate constant k decreases with increase in the initial concentration of 3-AP. This finding indicates that the degradation kinetics of 3-AP is not of simple first-order but pseudo-first-order.

It was also observed from the slopes of the lines in Fig. 3 that the degradation rate constant decreases rapidly at low initial 3-AP concentrations, then begins to change slowly as the initial concentration increases. As it can be seen from the values given in Table 1, the change in the rate constant is 1.47×10^{-3} min^{-1} when the initial 3-AP concentration increases from 6.0×10^{-5} to 7.6×10^{-5} mol l^{-1}. However, when the initial concentration increases from 10.5×10^{-5} to 12.6×10^{-5} mol l^{-1}, the decrease in the rate constant is 0.50×10^{-3} min^{-1}.

The reason for this initial concentration dependence of the photodegradation rate of 3-AP is that the degradation reaction occurs on TiO_2 particles as well as in solution [18]. On the photocatalyst surface, the reaction occurs between the $^{\bullet}OH$ radicals generated at the active OH^- sites and a 3-AP molecule from the solution. Thus, when the initial concentration is high, the number of these available active sites is decreased by 3-AP molecules, because of their competitive adsorption on TiO_2 particles, and rate of transfer of 3-AP from the solution does not affect the degradation rate. But, when the initial 3-AP concentration is low, transfer rate plays an important role. From Fig. 4, it can be seen that the degradation rate constants obtained in this study are proportional to the reciprocal of the initial 3-AP concentration. The correlation constant for the fitted line is 0.9979. Wei and Wan [9] have obtained a similar result for the photodegradation of phenol.

Table 1
Effect of initial concentration of 3-AP on the photodegradation rate

C_0 (10^{-5} mol l^{-1})	k (10^{-3} min^{-1})	r
6.0	7.69 ± 0.28	0.9941
7.6	6.22 ± 0.18	0.9963
8.9	5.66 ± 0.09	0.9990
10.5	5.06 ± 0.16	0.9953
12.6	4.56 ± 0.05	0.9960

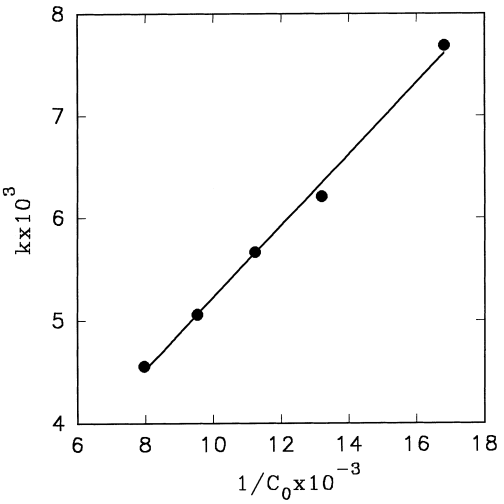

Fig. 4. Plot of the apparent rate constant vs. the reciprocal of the initial 3-AP concentration.

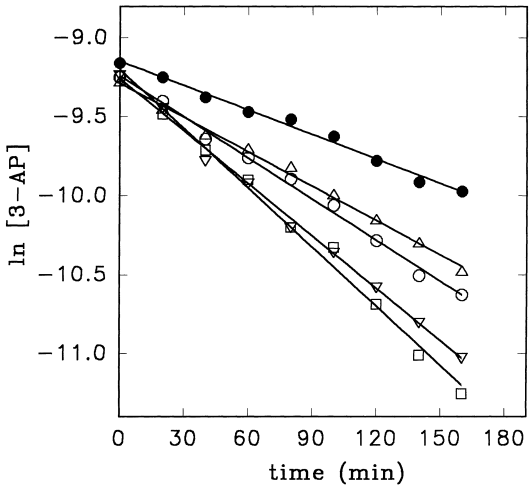

Fig. 5. Effect of H_2O_2 addition on the photodegradation rate of 3-AP ((●) without H_2O_2, (△) 0.5×10^{-3} mol l^{-1}, (○) 1.0×10^{-3} mol l^{-1}, (▽) 1.5×10^{-3} mol l^{-1}, (□) 2.0×10^{-3} mol l^{-1}).

3.4. Effect of electron acceptors

The photocatalytic degradation of organic compounds depends upon their reactions with $^{\bullet}$OH radicals. Based on this fact, it has been suggested that the addition of electron acceptors into the reaction solution enhances the degradation rates, since they generate $^{\bullet}$OH radicals [19–21].

3.4.1. Effect of H_2O_2

The effect of H_2O_2 has been investigated in numerous studies and observed that it increases the photodegradation rates of organic pollutants [9,10,22]. The added H_2O_2 reacts with conduction band electrons e^-_{CB} to generate $^{\bullet}$OH radicals which are necessary for the photodegradation;

$$H_2O_2 + e^-_{CB} \rightarrow {}^{\bullet}OH + OH^- \quad (1)$$

H_2O_2 does not only generate $^{\bullet}$OH radicals, but it also inhibits e^-–h^+ recombination process at the same time, which is the most practical problem in using TiO_2 as a photocatalyst.

In this study, the variation in the photodegradation rate of 3-AP was determined as a function of H_2O_2 concentration over the range of $(0.5–2.0) \times 10^{-3}$ mol l^{-1} at pH $= 5.3 \pm 0.2$ and at a constant temperature of $22 \pm 2^{\circ}$C by using suspensions at 1.0×10^{-4} mol l^{-1} 3-AP concentration. The results are presented in Fig. 5 and in Table 2. As it can be seen from the straight lines obtained, the photocatalytic degradation of 3-AP with the addition of H_2O_2 also follows the pseudo-first-order kinetics. Furthermore, they also show that the addition of H_2O_2 enhances the degradation rate of 3-AP, as expected. The apparent rate constant was also found to be dependent upon the concentration of H_2O_2, $[H_2O_2]$. The k values, tabulated in Table 2, increase as the concentration of H_2O_2 increases. In order to find the order of $[H_2O_2]$ dependence of the photodegradation of 3-AP, the apparent rate constant was expressed as

$$k = k'[H_2O_2]^{\alpha} \quad (2)$$

in light of the results of an earlier work on the photodegradation of phenol [9]. The order of this dependence α was calculated to be 0.400 by linear regression. In a previous study, we calculated the same order to be equal to 0.364 for aniline [16], whereas Wei and Wan [9] have obtained 0.500 for phenol which is of the same order of magnitude.

3.4.2. Effect of $K_2S_2O_8$ and $KBrO_3$

The $K_2S_2O_8$ and $KBrO_3$ are efficient electron acceptors and used as additives to enhance the photodegradation rates [19–21]. They readily react with conduction band electrons and rapidly dissociate into harmless products. They also lead to the formation of $^{\bullet}$OH radicals. The persulphate ion accepts an electron and dissociates into a sulphate ion and

$$S_2O_8{}^{2-} + e^-_{CB} \rightarrow SO_4{}^{2-} + SO_4{}^{-\bullet} \quad (3)$$

a sulphate ion radical. The $SO_4{}^{-\bullet}$, thus formed, then reacts with a water molecule and generates $^{\bullet}$OH radicals.

$$SO_4{}^{-\bullet} + H_2O \rightarrow SO_4{}^{2-} + {}^{\bullet}OH + H^+ \quad (4)$$

The bromate ion also accepts electrons and dissociates into bromide ions according to the equation

$$BrO_3{}^- + 6\,e^- + 6\,H^+ \rightarrow Br^- + 3\,H_2O \quad (5)$$

Table 2
Effect of H_2O_2 on the photodegradation of 3-AP

$[H_2O_2]$ (10^{-3} mol l^{-1})	k (10^{-3} min^{-1})	r
0.0	5.06 ± 0.16	0.9953
0.5	7.24 ± 0.19	0.9976
1.0	8.66 ± 0.24	0.9973
1.5	11.06 ± 0.25	0.9982
2.0	12.49 ± 0.41	0.9963

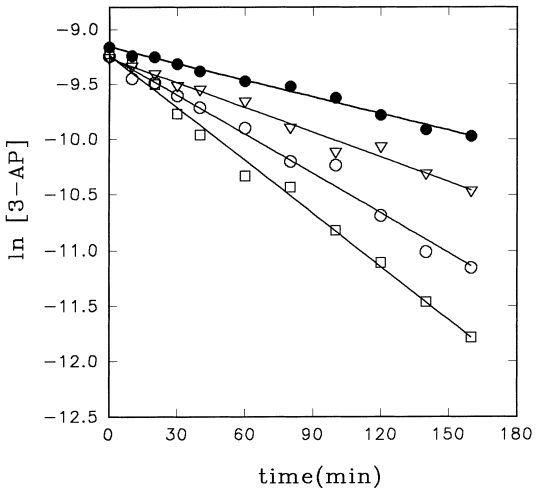

Fig. 6. Effect of electron acceptors on the photodegradation rate of 3-AP ((●) without additive, (▽) with $K_2S_2O_8$, (○) with H_2O_2, (□) with $KBrO_3$).

Since both of the compounds react with electrons, they also inhibit e^-–h^+ recombination process and prolong the life-time of the photogenerated holes.

In this study, the effects of $K_2S_2O_8$ and $KBrO_3$ on the photodegradation rate of 3-AP were investigated by using suspensions at 1.0×10^{-4} mol l^{-1} 3-AP concentration at a constant temperature of 22 ± 2°C. The concentration of the additives was 2.0×10^{-3} mol l^{-1} and the initial pH of the reaction solution was 5.3 ± 0.2. The experimental results are presented in Fig. 6 and Table 3. The results show that the photocatalytic degradation of 3-AP with the addition of $K_2S_2O_8$ and $KBrO_3$ also follows the pseudo-first-order kinetics. For comparison, the results obtained for the photodegradation of 3-AP in the presence of 2.0×10^{-3} mol l^{-1} H_2O_2 with the initial 3-AP concentration of 1.0×10^{-4} mol l^{-1} are also given in Fig. 6 and Table 3. It can be seen from the values given in Table 3 that the addition of $K_2S_2O_8$ improves the photodegradation of 3-AP. The rate constant increased from 5.06×10^{-3} to 7.48×10^{-3} min^{-1} upon the addition of 2.0×10^{-3} mol l^{-1} $K_2S_2O_8$. The H_2O_2 appears to be more effective than $K_2S_2O_8$. The rate constant further increased to 12.49×10^{-3} min^{-1} when H_2O_2 was used instead of $K_2S_2O_8$. Further improvement was obtained with $KBrO_3$; the rate constant increased to 15.76×10^{-3} min^{-1} upon the addition of 2.0×10^{-3} mol l^{-1} $KBrO_3$.

Table 3
Effect of electron acceptors on the photodegradation rate of 3-AP (initial concentration of 3-AP is 1.0×10^{-4} mol l^{-1})

Electron acceptor[a]	k (10^{-3} min^{-1})	r
Without additive	5.06 ± 0.16	0.9953
$K_2S_2O_8$	7.48 ± 0.38	0.9914
H_2O_2	12.49 ± 0.41	0.9963
$KBrO_3$	15.76 ± 0.47	0.9969

[a] Initial concentration of each electron acceptor is 2.0×10^{-3} mol l^{-1}.

Thus, we may conclude that $KBrO_3$ is the most effective electron acceptor for the photodegradation of 3-AP, among the three additives studied. The reason can be attributed to the number of electrons it reacts as shown in Eq. (5).

3.5. Prediction of the primary intermediates

In aqueous TiO_2 suspensions, aromatic compounds are oxidized through two different mechanisms; either by hydroxylation of the aromatic ring [7–9]

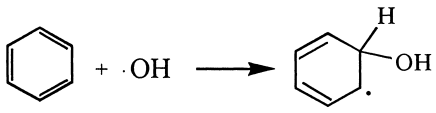

(6)

or by direct electron transfer to TiO_2 followed by the addition of a water molecule and loss of a proton [23–25];

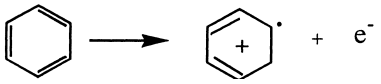

(7)

In both of the reaction paths, a hydroxycyclohexadienyl radical is formed. The subsequent reactions of these intermediates lead to the mineralization of the aromatic compounds. The photodegradation reactions of organic pollutants may take place through formation of harmful intermediates that are more toxic than the original compounds. Therefore, knowledge on the identities of the intermediates is a necessity in photocatalytic degradation processes.

In this study, in order to predict the primary intermediates, the kinetics of the hydroxylation reaction of 3-AP was investigated theoretically. Since the same intermediate is formed in both of the above mentioned oxidation paths, the photocatalytic degradation of 3-AP may be based on hydroxyl radical chemistry. Hydroxyl radical has a strong electrophilic character [26], it attacks to one of the carbon atoms of the aromatic ring, generally the one with the highest electron density. Four different reaction paths for the hydroxylation of 3-AP were determined by the nature of the carbon atoms of the aromatic ring. In all of the possible reaction paths, shown in Fig. 7, the •OH radical attacks a carbon atom with its unpaired electron and upon contact forms a C–O bond, while a π-bond of the aromatic system is broken and a hydroxylated radical is formed. In order to predict the primary intermediates, the equilibrium structures, electronic and thermodynamic properties of the reactants, 3-AP and •OH, four different hydroxylated radicals formed and the corresponding transition state TS structures were evaluated by quantum mechanical calculations.

Geometry optimizations were performed with the semiempirical PM3 method within the MOPAC 6.0 package [27]. The molecular orbital calculations were carried out by a self-consistent field SCF method using the restricted RHF or unrestricted UHF Hartree-Fock formalisms depending upon the multiplicity of each species. The molecular models were created by using the mean bond distances,

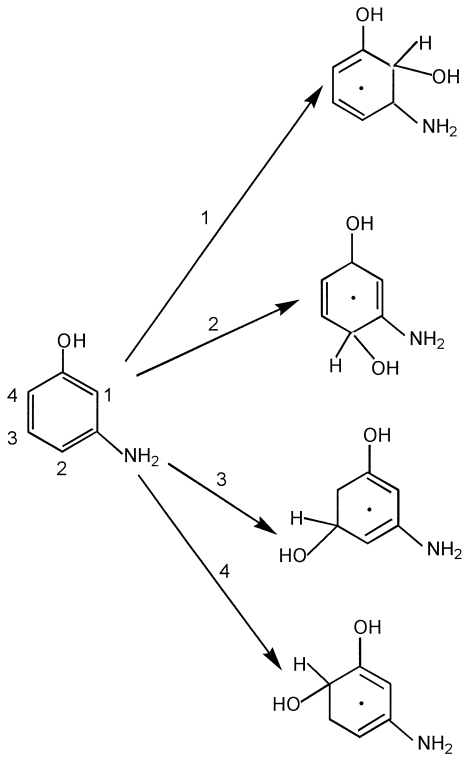

Fig. 7. Possible reaction paths for the hydroxylation of 3-AP.

the benzene ring, tetrahedral angles for sp^3-hybridized nitrogen and oxygen atoms and 120° for sp^2-carbons. These structures were input coordinates for PM3 calculations. The criterion for terminating all optimizations was increased by using the PRECISE option. Vibrational frequencies were calculated for the determination of the reactant and the product structures as stationary points and true minima on the potential energy surfaces using the keyword FORCE. All the stationary points were confirmed by the presence of positive vibrational frequencies. For a stationary point, the first derivatives of the energy with respect to changes in the geometry are zero. Whereas, the criterion for a minimum is that all eigenvalues of the Hessian matrix are positive [28]. The forming C–O bond was chosen as the reaction coordinate in the determination of the transition states and each transition state was characterized with only one negative eigenvalue in its force constant matrix.

The optimized structures obtained for the four transition states are presented in Fig. 8. The major structural changes relative to 3-AP are localized around the carbon atom to which the •OH radical attacks. Upon the approach of •OH, this carbon atom moves slightly out of the plane of the ring. The dihedral angles calculated are in the range of 0.5–0.9°. The coming oxygen atom makes a 104.1–109.8° angle with the C–C bond, while the hydrogen atom moves out of the

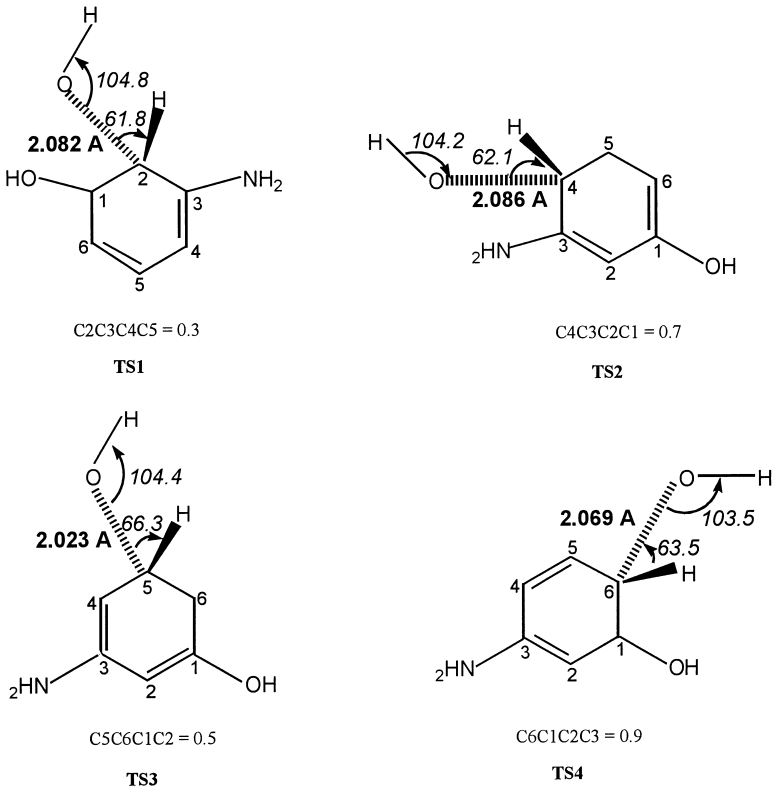

Fig. 8. Optimized structures for the transition states.

Table 4
Predictors for the determination of the most probable TS

Path	C–O (A°)	n_{C-O}	ΔH_f(kcal/mol)
1	2.082	0.143	−17.310
2	2.086	0.138	−17.566
3	2.023	0.172	−15.716
4	2.069	0.145	−17.123

Table 5
Kinetic parameters for the four possible reaction paths

Path	E_a (kcal/mol)	k ($cm^3 \cdot$ molecule^{-1} s^{-1})	ΔH_r (kcal/mol)
1	3.860	1.124×10^{-15}	−37.637
2	3.607	5.763×10^{-15}	−37.015
3	5.443	1.055×10^{-16}	−33.653
4	4.094	2.915×10^{-15}	−36.326

plane of the ring. The dihedral angles calculated for the hydrogen atom are greater than the ones obtained for the carbon atom; 5.1–8.8°. These findings indicate that the carbon atom to which •OH is bonded changes from sp^2- to sp^3-hybridized. Three predictors were determined for the prediction of the most probable TS; the length of the forming C–O bond, its bond order n_{C-O} and the heat of formation of the TS, ΔH_f. They are presented in Table 4. The C–O bond length is a sensitive measure for the formation of the transition state along the reaction coordinate. As it can be seen from the values given in Fig. 8 and in Table 4, the longest C–O bond belongs to TS2. This suggests that TS2 is the earliest transition state and is in clear agreement with the smallest bond order n_{C-O}, which is 0.138 as presented in Table 4. Furthermore, TS2 has the lowest heat of formation among the four transition state structures, indicating that this is the most thermodynamically stable, and thus, the most probable transition state structure.

The rate constant k for each reaction path was calculated by using the Transition State Theory over a temperature range of 200–400 K. The classical rate constant k in Transition State Theory is

$$k = \frac{kT}{h}\frac{q_{TS}}{q_{AP}q_{OH}}e^{-E_a/RT} \quad (8)$$

where k is Boltzman's constant, T the temperature, h the Planck's constant, q's are the molecular partition functions for TS and the reactant species, 3-AP and •OH, and E_a is the activation energy. Each of the molecular partition functions was assumed to be the product of translational, rotational, vibrational and electronic partition functions of the corresponding species. The activation energies for the four reaction paths were calculated as the difference between the heats of formation of the transition state complexes and the sum of the heats of formation of the reactants. The calculated rate constants k, activation energies E_a and heats of reaction ΔH_r, calculated as the sum of the heats of formation of the products minus the sum of the heats of formation of the reactants are presented in Table 5. As it can be seen from the values, the lowest activation energy and the highest rate constant belongs to path 2. This result is consistent with Hammond's postulate [29] stating that early transition states have low energy barriers and high exothermicities. Arrhenius plots of the four possible reaction paths, shown in Fig. 9, also support this finding. Path 2 proceeds faster than the three possible reaction paths. Thus, we may conclude that the most probable primary intermediate that forms in the photodegradation

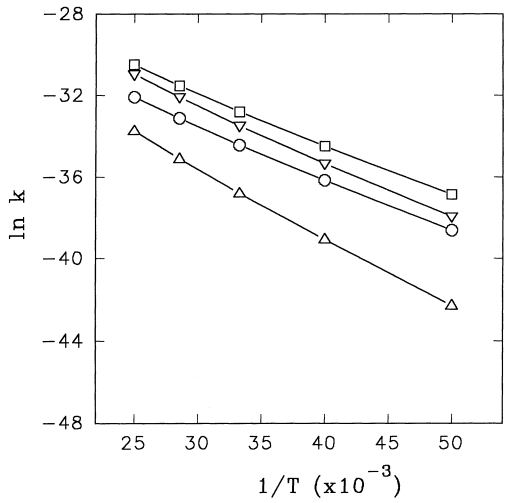

Fig. 9. Arrhenius plots for the four possible reaction paths ((○) path 1, (□) path 2, (△) path 3, (▽) path 4).

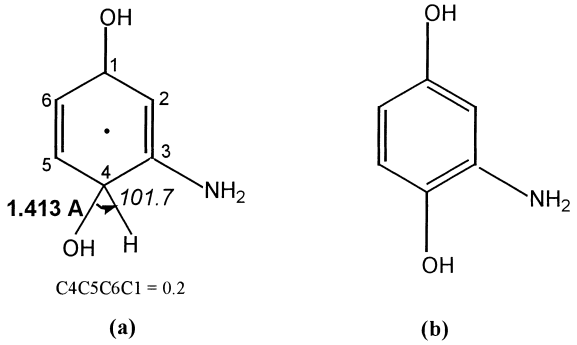

Fig. 10. Primary intermediates of the photodegradation of 3-AP.

of 3-AP is 1,4-dihydroxy-3-amino-cyclohexa-2,5-dienyl radical which then forms 2-aminohydroquinone, shown in Fig. 10a and b, respectively. The relative concentration of this product was calculated to be 58.2%. A second probable intermediate, 1,6-dihydroxy-3-amino-cyclohexa-2,4-dienyl radical also forms with a relative concentration of 29.4%.

4. Conclusion

The results of this study show that the photocatalytic degradation of 3-AP in aqueous TiO_2 suspensions follows

a pseudo-first-order kinetics. The apparent rate constant depends on the initial 3-AP concentration. A linear dependence of the rate constant upon the reciprocal of the initial 3-AP concentration has been obtained. The addition of electron acceptors; H_2O_2, $K_2S_2O_8$ and $KBrO_3$ enhances the reaction rate significantly. The order of the dependence of the rate constant on H_2O_2 concentration has been calculated to be 0.400. Based on the results of the quantum mechanical calculations, the most probable primary intermediate has been determined to be 1,4-dihydroxy-3-amino-cyclohexa-2,5-dienyl radical which then forms 2-aminohydroquinone.

Acknowledgements

The authors greatly appreciate Yıldız Technical University Research Fund for financial support (Project No:20-01-02-03) and Degussa Limited Company Turkey for the generous gift of TiO_2 P25.

References

[1] A. Mills, S. Le Hunte, J. Photochem. Photobiol. A: Chem. 108 (1997) 1.
[2] D. Bahnemann, J. Cunningham, M.A. Fox, E. Pelizzetti, P. Pichat, N. Serpone, in: G.R. Helz, R.G. Zepp, D.G. Crosby (Eds.), Aquatic and Surface Photochemistry, Lewis, Baco Raton, FL, 1994, p. 261.
[3] P. Pichat, in: G. Ertl, H. Knözinger, J. Weitkamp (Eds.), Handbook of Heterogeneous Photo-catalysis, Vol. 4, VCH, Weinheim, 1997, p. 2111.
[4] D.F. Ollis, E. Pelizzetti, N. Serpone, Environ. Sci. Technol. 25 (9) (1991) 1523.
[5] D.W. Bahnemann, D. Bockelmann, R. Goslich, Sol. Energy Mater. 24 (1991) 564.
[6] J.C. D'Oliveira, C. Minero, E. Pelizzetti, P. Pichat, J. Photochem. Photobiol. A: Chem. 72 (1993) 261.
[7] R.W. Matthews, S.R. McEvoy, J. Photochem. Photobiol. A: Chem. 64 (1992) 231.
[8] S. Das, M. Muneer, K.R. Gopidas, J. Photochem. Photobiol. A: Chem. 77 (1992) 83.
[9] Y.T. Wei, C. Wan, J. Photochem. Photobiol. A: Chem. 69 (1992) 241.
[10] Y.T. Wei, Y.Y. Wang, C. Wan, J. Photochem. Photobiol. A: Chem. 55 (1990) 115.
[11] J.C. D'Oliveira, G. Al-Sayyed, P. Pichat, Environ. Sci. Technol. 24 (1990) 990.
[12] A. Huang, L. Cao, J. Chen, F.J. Spiess, S.L. Suib, T.N. Obee, S.O. Hay, J.D. Freihaut, J. Catal. 188 (1999) 40.
[13] U. Stafford, K.A. Gray, P. Kamat, J. Catal. 167 (1997) 25.
[14] C. Minero, E. Pelizzetti, P. Piccini, M. Vincenti, Chemosphere 28 (1994) 1229.
[15] M.S. Dieckmann, K.A. Gray, Wat. Res. 30 (1996) 1169.
[16] N. San, Z. Çinar, Toxicol. Environ. Chem. 79 (2001) 179.
[17] J.G. Calvert, J.N. Pitts, Photochemistry, Wiley, New York, 1966, pp. 783–786.
[18] H. Al-Ekabi, P. De Mayo, J. Phys. Chem. 90 (1986) 4075.
[19] H. Al-Ekabi, B. Butters, D. Delary, J. Ireland, N. Lewis, T. Powell, J. Story, in: D.F. Ollis, H. al-Ekabi (Eds.), Photocatalytic Purification and Treatment of Water and Air, Elsevier, Amsterdam, 1993, pp. 321–335.
[20] I. Paulios, I. Tsachpinis, J. Chem. Technol. Biotechnol. 74 (1999) 349.
[21] L. Sanchez, J. Peral, X. Domenech, Appl.Catal. B: Environ. 19 (1998) 59.
[22] M. Halmann, J. Photochem. Photobiol. A: Chem. 66 (1992) 215.
[23] R.B. Draper, M.A. Fox, Langmuir 6 (1990) 1396.
[24] G. Lu, A. Linsebigler, J.T. Yates Jr., J. Phys. Chem. 99 (1995) 7626.
[25] L. Cermenati, P. Pichat, C. Guillard, A. Albini, J. Phys. Chem. B 101 (1997) 2650.
[26] V. Brezova, M. Ceppan, E. Brandsteterova, M. Breza, L. Lapcik, J. Photochem. Photobiol. A: Chem. 59 (1991) 385.
[27] J.P. Stewart, MOPAC QCPE Program, 455, Bloomington, Ind., 1990.
[28] M.W. Jurema, G.C. Shields, J. Comp. Chem. 14 (1993) 89.
[29] W.J. Hehre, L. Radom, P.R. Schleyer, J.A. Pople Ab Initio Molecular Orbital Theory, Wiley, USA, 1986.